

## Electrochemical Properties of Nanotubes and Nanomicelles from Novel Polyaniline and Derivative

Michael J. Klink<sup>1</sup>, E.I. Iwuoha<sup>2</sup>, Eno E. Ebenso<sup>1,\*</sup>

<sup>1</sup> Department of Chemistry, School of Mathematical and Physical Sciences, North-West University (Mafikeng Campus), Private Bag X2046, Mmabatho 2735, South Africa

<sup>2</sup> Sensor Research Laboratory, Department of Chemistry, University of the Western Cape, Private Bag X17, Bellville, 7535, South Africa

\*E-mail: [Eno.Ebenso@nwu.ac.za](mailto:Eno.Ebenso@nwu.ac.za)

*Received:* 14 February 2012 / *Accepted:* 22 March 2012 / *Published:* 1 April 2012

---

Phenanthrene sulfonic acid (PSA) and anthracene sulfonic acid (ASA) were incorporated into Polyaniline (PANI), poly (2,5 dimethoxyaniline) (PDMA) and poly(o-methoxyaniline) (POMA) backbones, respectively. UV-Vis and FTIR spectra indicated the incorporation of PSA and ASA into PANI, PDMA and POMA backbones. The SEM micrographs showed well defined polymeric nanotubes with diameters between 50 to 100 nm for PSA doped PDMA. Nanomicellular structures were formed by PSA doped POMA with radius between 100 to 200 nm. Cyclic voltammetric characterization of the polymer pastes showed distinctive redox peaks, which indicates that the polymer films on the Pt electrode were electroactive and the redox state can be electrochemically controlled.

---

**Keywords:** Phenanthrene Sulfonic Acid, Anthracene Sulfonic Acid, Polyaniline nanotubes, Poly(2,5 dimethoxyaniline), Poly(ortho-methoxyaniline), Nano-micelles

### 1. INTRODUCTION

Material science has been part of our lives ever since the ancient stone, bronze, iron, steel, and silicon ages [1-3]. It has improved our lives through design and creation of new materials most importantly because the modern era lifestyle requires or rather really depends on material that is of high degree of sophistication [2,3]. This sophisticated materials are used in technology that adds convenience to our lives thus, the properties of materials should be improved and the only way to accomplish that is through imaginative molecular design and synthesis of new materials [1]. The

challenges of designing and creating new, reproducible, and diverse materials are the consumer market, demands to lifestyle improvement [2], and limitations of environmental protection and public safety [3].

Research activities in organic conducting polymers have been studied extensively for their unique electrical and physical properties, chemical stability, low cost and potential technological application over the last decade [4,5]. Of interest are conducting polyaniline polymers, for example poly (2,5 dimethoxyaniline) (PDMA) and poly (ortho-methoxyaniline) (POMA), which are capable of incorporating different functionalities in their matrix during or after polymerisation. These conducting polymers have conjugated  $\pi$ -electron backbones, which display unusual properties such as low-energy optical transitions, low ionisation potentials and high electron affinities. This results in a class of polymers that can be oxidised or reduced more readily and more reversibly than conventional polymers [6–8].

The synthesis of nanomaterials was mainly for potential use in catalysis and electronics. A lot of interest has focused on enhancing the properties of these materials by changing their surface properties [9,10]. The change in surface properties is commonly achieved by surrounding a conductive polymer by another material, usually a bulky dopant. This forces the polymer backbone to the inside of the molecule forming different nanostructures including nanotubes and nanomicelles. Conducting polymers synthesised in the form of nanotubes and micelles are of particular interest since their properties significantly differ from the properties of corresponding macroscopic materials [11].

In the present work, phenanthrene sulfonic acid (PSA) and anthracene sulfonic acid (ASA) have been incorporated into the polyaniline (PANI), poly (2,5 dimethoxyaniline) [PDMA] and poly (ortho-methoxyaniline) [POMA] backbones. Electrochemical and morphological techniques were used to characterize the properties of these polymers.

## 2. EXPERIMENTAL

### 2.1 Materials

Phenanthrene sulfonic acid and anthracene sulfonic acid were chemically synthesized in the laboratory. Reagents aniline, 2,5 dimethoxyaniline, ortho-methoxyaniline (or o-anisidine), phenanthrene, anthracene and potassium bromide were obtained from Aldrich (Germany). Fluka (Germany) supplied the dimethyl sulfoxide, dimethyl ether and ammonium persulfate. Merck's hydrochloric acid and methanol were used in the experiments. All reagents were purchased in Cape Town (South Africa), were of analytical grade and were used as obtained without further purification.

### 2.2 Synthesis

#### 2.2.1 Synthesis of phenanthrene- and anthracene sulfonic acid

A 10 ml of fuming  $\text{H}_2\text{SO}_4$  was diluted with 10 ml 6 M  $\text{H}_2\text{SO}_4$  and the mixture was diluted to 100 ml in a volumetric flask. 50 ml of the above solution was added to a round bottom flask that

contained 2 g of phenanthrene. The contents were heated to boiling in an oil bath (temperature between 100 – 140 °C) fitted with a condenser and thermometer. The mixture was refluxed for 3 hr with constant stirring. The mixture was then poured into crushed ice for 20 minutes and the unreacted phenanthrene was filtered off. 10 ml of a 50% NaOH was added to the mixture and put in a refrigerator to crystallize forming a white phenanthrene sulfonic salt. The salt was then hydrolysed to form the phenanthrene sulfonic acid (fig. 1). The same procedure was followed for the synthesis of anthracene sulfonic acid [12].

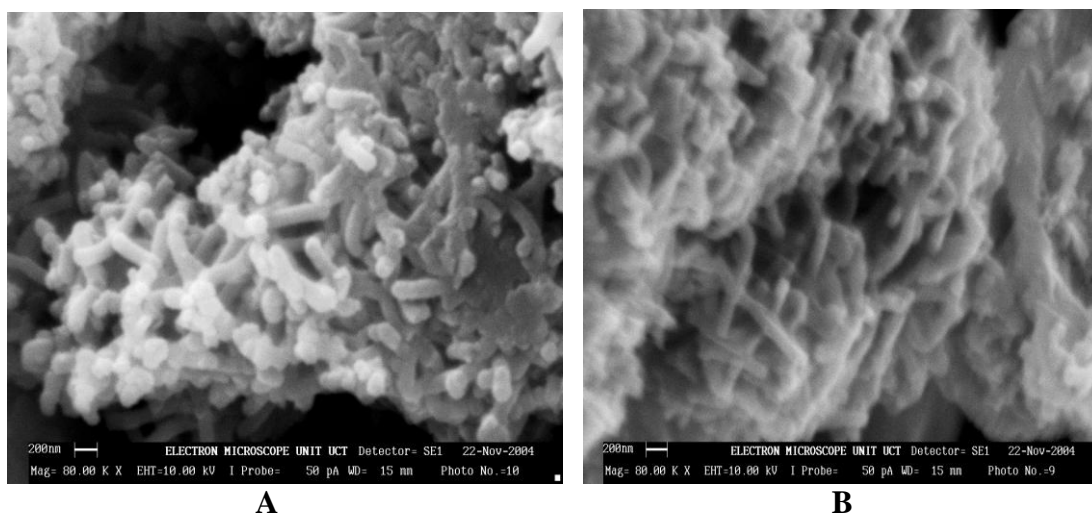


**Figure 1.** SEM images of PANI/PSA (a) and PANI/PSA (b) at different magnifications

### 2.2.2. Synthesis of polyaniline/phenanthrene- and anthracene sulfonic, poly (2,5 dimethoxyaniline)/phenanthrene- and anthracene sulfonic acid nanostructures and poly (o-methoxyaniline)/phenanthrene- and anthracene sulfonic acid nanostructures

A 2,5 dimethoxyaniline (0.0334 g), 20 ml of deionized water and phenanthrene sulphonic acid (0.2592 ml) were placed in a 100 ml beaker. The mixture was heated for 30 min at 50 °C while stirring vigorously. An aqueous solution of ammonium persulphate (APS) (0.1 M) was added dropwise to the hot solution. The mixture was cooled down to room temperature while continuously stirred for 15 hr. The product was filtered and washed with deionised water, methanol and dimethyl ether 3 times respectively, to remove impurities such as APS, free ASA and unreacted 2,5 dimethoxyaniline. The same procedure were used for the synthesis of polyaniline/phenanthrene and poly (o-dimethoxyaniline)/phenanthrene sulfonic acid nanostructures, except that 0.26 ml of aniline and *ortho*-methoxyaniline (o-anisidine) were used in place of 2,5 dimethoxyaniline. The same procedure was followed for the synthesis of anthracene sulfonic acid derivatives [6, 7].

### 2.3 Instrumentation

Scanning electron microscopy (SEM) was performed with a Hitachi X650 scanning electron microscope. UV/Vis absorbance measurements were recorded at room temperature on a UV/Vis 920

spectrometer (GBC Scientific Instruments, Australia) and the FTIR measurements were recorded as a mixture of KBr (99%) and sample (1%) pellet using a Perkins Elmer, Paragon 1000 PC, FTIR spectrometer. All electrochemical experiments were performed with and recorded on a BAS50/W electrochemical analyser (Bioanalytical Systems, Lafayette, IN, USA). Alumina micropolish and polishing pads (Buehler, IL, USA) were used for electrode polishing.

#### 2.4 Electrochemical measurements

A conventional three electrode system was employed: working (WE) was a platinum disc electrode, silver/silver chloride (Ag/AgCl) and a platinum gauze were used as reference and auxiliary electrodes, respectively. A paste of the different polymers (0.4 g) in 2 ml HCl (1 M) were first prepared and degassed with argon for 20 minutes to exclude any oxygen from the paste. For convention, a negative oxidation current was used for the display of all figures.

### 3. RESULTS AND DISCUSSION

#### 3.1. Spectroscopic Characterisation

##### 3.1.1. Scanning Electron Microscopy

The morphology and structure of monomers PANI, PDMA and POMA doped with PSA and ASA were investigated. It is generally agreed upon that morphology of the resultant polymers can be as diverse as there are main polymer chains, dopant structure, synthetic routes and conditions [13]. When PANI was doped with ASA and PSA nanostructures were observed (figure 1). In micrograph (a) tubes or fibres can be seen when PANI was doped with ASA with diameter between 50 – 100 nm at 80 000 x magnification.

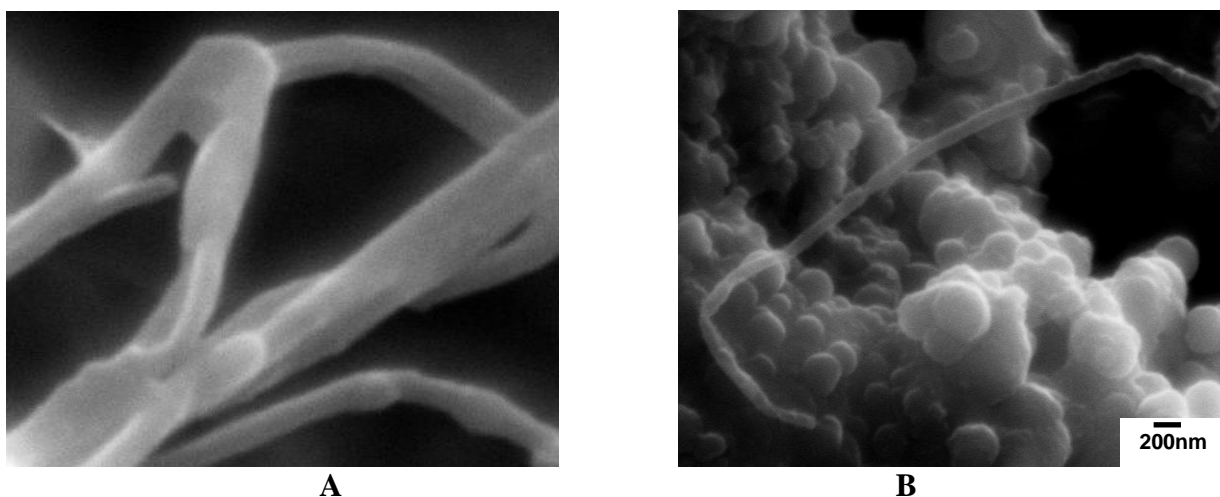


**Figure 2.** SEM images of PDMA/PSA (a) and POMA/PSA (b) at different magnifications

Nanotubes or fibres were also observed when PANI was doped with PSA (b) with observed diameters between 50 and 100 nm (80 000 x magnification). It is clearly seen that the surface is covered with fibres interconnected with each other showing net-like features [5, 13, 14].

Figure 2 shows SEM micrographs of PDMA and POMA with PSA. The effect of the different dopants on the monomers, prepared under the same conditions, was clearly observed in the SEM images. In micrograph (a) PDMA doped with PSA formed nanotubes or nanofibres with diameter between between 50 and 100 nm. However, when POMA was doped with PSA in (b) micelle (egg-like) structures and disc-like formations with cross sectional diameter in the 100 to 200 nm range were formed. This might be a result of POMA, which is hydrophobic, being forced inside and the bulky groups of phenanthrene sulfonic acid, which is hydrophilic, on the outside in the micelle formation. Flat round, disc-like formations were seen (40 000 x magnification) when PDMA and POMA were doped with ASA (not shown), which could be the effect of the different isomers of PSA formed during synthesis [8, 13, 15].

### 3.1.2 UV-Vis spectroscopy

UV-vis spectroscopy gives information regarding the doping of PANI, POMA and PDMA with the sulfonic acids. The doping of PANI with ASA (not shown) have absorption bands at 320 nm, assigned to the  $\pi$ - $\pi^*$  transitions of the benzoid structure, at 700 nm due to the exciton absorption of the quinoid structure and at 440 nm due to an intermediate state formed during the electro-oxidation of the leucoemeraldine form of PANI.

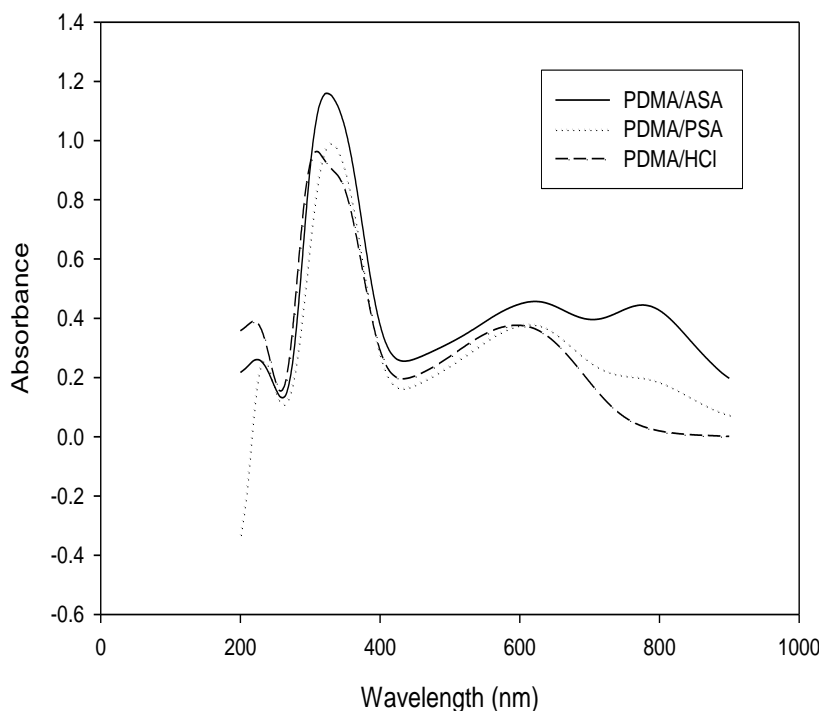


**Figure 3.** UV-visible absorption spectra of PDMA/ASA, PDMA/PSA and PDMA/HCl

The band at 450 nm is due to the charged para-coupled phenyl structures and corresponds to phenyl excitons or polarons [16, 17]. Shoulder bands between 200 – 300 nm are assigned to unreacted PANI and ASA in solution. Similar absorption bands were seen for PANI doped with PSA (not shown) with bands at 320 nm, 420 nm and 675 nm [18, 19, 20].

The UV-vis absorption spectra of PDMA doped with PSA (figure 3) showed 3 absorption bands at wavelengths, 350, 600 and 800 nm respectively. The band at 350 nm corresponds to the reduced state (leucoemeraldine) of PDMA and it is due to  $\pi$ - $\pi^*$  transition. The band at 600 nm corresponds to partial oxidation of PDMA and can be assigned to represent the intermediate state between leucoemeraldine form containing benzenoid rings and emeraldine form containing conjugated quinoid rings in the backbone of the PDMA (polaron).

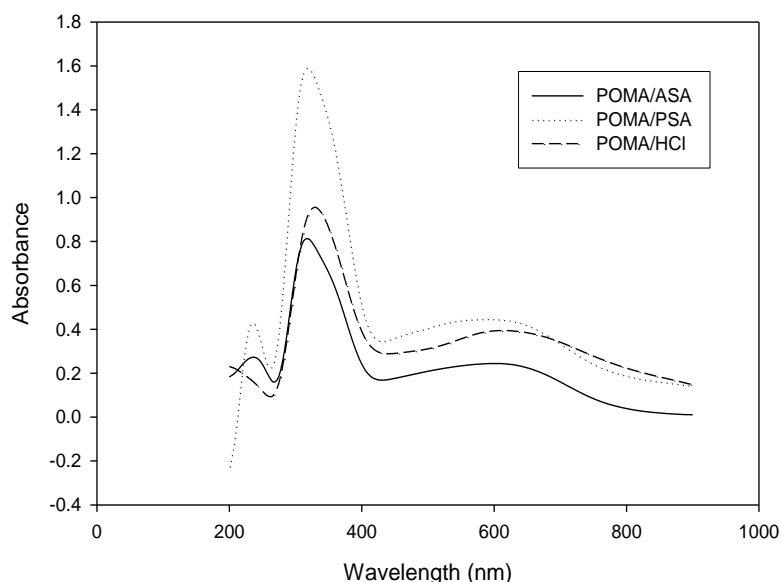


**Figure 4.** UV-visible absorption spectra of POMA/ASA, POMA/PSA and POMA/HCl

The emeraldine form transforms into fully oxidized pernigraniline form characterized by a broadened band at around 800 nm (bipolaron). The band at around 800 nm was not seen for PDMA doped with HCl [21-22]. The UV-vis absorption spectrum of POMA doped with PSA (Figure 4) is dominated by 2 absorption bands at 2 selected wavelengths, 350 and 650nm respectively. The same absorption bands were seen for POMA doped with HCl. These bands are associated with  $\pi$ - $\pi^*$  transition and polaron forms of POMA. This confirmed that the POMA polymers and POMA/HCl are doped but not as high as when the bipolaron forms are present, shown in PDMA polymers [19].

### 3.1.3 FTIR spectroscopy

FT-IR has provided valuable information regarding the formation of the sulfonic acids and PANI, POMA and PDMA polymers doped with the sulfonic acids.

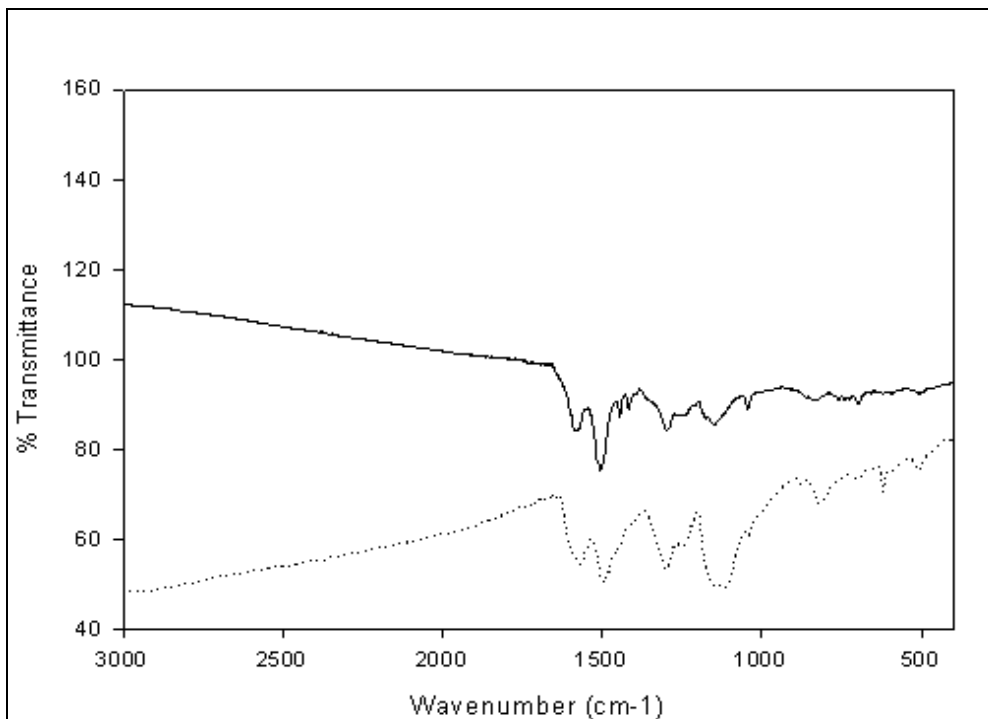


**Figure 5.** FT-IR spectra of (—) PANI-PSA and (.....) PANI-ASA

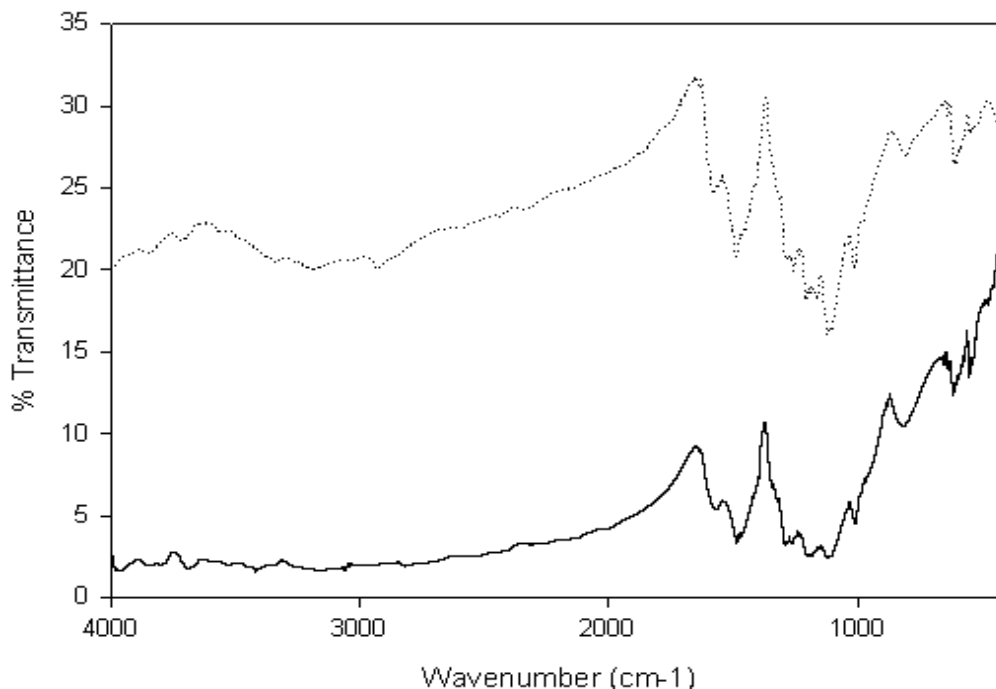


**Figure 6.** FT-IR spectra of (—) POMA-ASA and (.....) POMA-PSA

Figure 5 gives the FT-IR spectra of PANI doped with ASA and PSA. The bands at  $1570\text{ cm}^{-1}$  for PANI/ASA and  $1595\text{ cm}^{-1}$  for PANI/PSA corresponds to the quinoid rings in the polymer backbone. The corresponding stretching vibration bands for the benzenoid rings occur at  $1480\text{ cm}^{-1}$

PANI/ASA and  $1495\text{ cm}^{-1}$  for PANI/PSA. The relatively strong bands at  $1300\text{ cm}^{-1}$  are assigned to the stretching vibrations of C-N in the quinoid imine units of both polymers [23, 24, 25].

The absorption peaks of POMA-ASA and POMA-PSA (figure 6) appear almost at the same wavenumbers as that of PANI doped with ASA and PSA, but with small shifts. The band at  $1600\text{ cm}^{-1}$  is associated with quinoid structure and  $1500\text{ cm}^{-1}$  band with benzenoid structure. The shifted quinone imine bands of POMA  $1600\text{ cm}^{-1}$ , indicate successful doping with ASA and PSA. The peaks at  $800\text{ cm}^{-1}$  in the POMA-ASA and POMA-PSA spectra are characteristic of an *ortho*- or *meta*-substituted aromatic rings and the appearance of the methoxy group which is *ortho* to the amino group. The band at  $1170\text{ cm}^{-1}$  is usually considered as a measure of delocalization of electrons on POMA and is referred to as the electronic like band, which is a characteristic peak of POMA conductivity [15, 24].

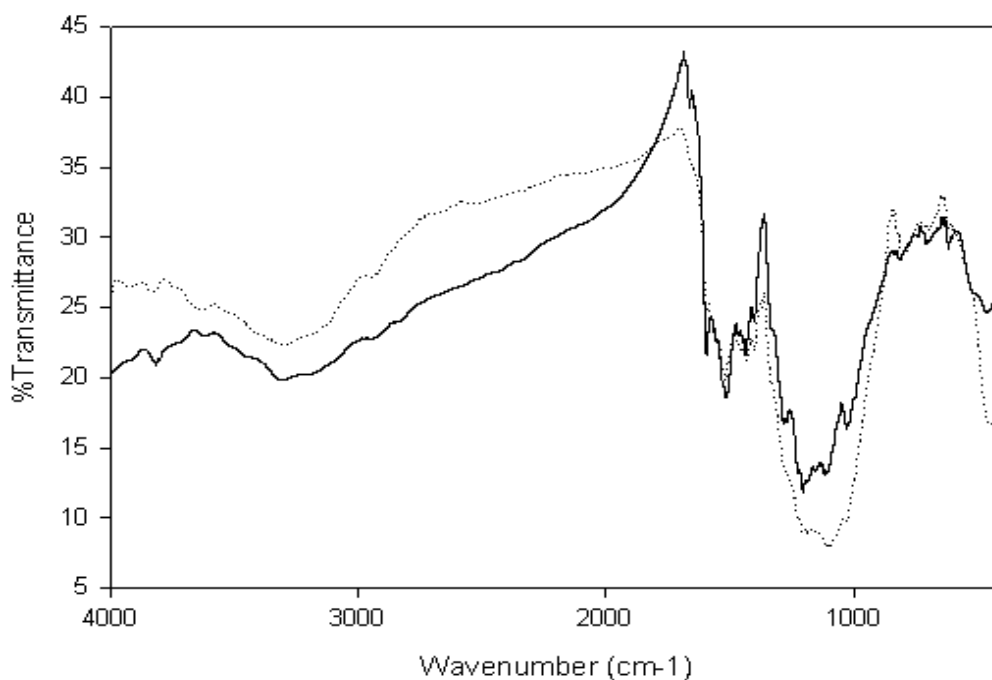


**Figure 7.** FT-IR spectra of (—) PDMA-ASA and (.....) PDMA-PSA

For PDMA/ASA (figure 7), the peaks of the quinoid units shift from  $1594$  and  $1152$  to  $1598$  and  $1159\text{ cm}^{-1}$  and the stretching vibrations of benzenoid ring to  $1465$  and  $1285\text{ cm}^{-1}$ . These shifts suggested changes of environment at the molecular level. The bands at  $1115$ ,  $1026$  and  $812\text{ cm}^{-1}$  are revealed to the 1-4 substitution on the benzene ring in PDMA. The absorption band around  $1080\text{ cm}^{-1}$  attributed to the presence of S=O stretching bands and confirms the existence of ASA in the polymer complex, suggests the incorporation of ASA into the polymer backbone. FTIR spectrum of PDMA doped PSA (figure 7) have absorptions between  $1600$  and  $1450\text{ cm}^{-1}$ , which are related to the stretching of C-N bonds of benzenic and quinonic rings in the polymer. Absorptions between  $1285$  and  $1154\text{ cm}^{-1}$  related to the asymmetric and symmetric stretching of =C-O-C bonds. The absorption band around  $1080\text{ cm}^{-1}$  attributes to the S=O group, also suggests the incorporation of PSA into the polymer backbone [11, 26].



### 3.2 Electrochemistry

#### 3.2.1 CV characterization of the polymers on platinum

The multi-scan rate voltammograms of PANI/ASA on Pt electrode in HCl (1M) solution with scan rates 5, 10, 15, 20, 30, 40 and 50 mV/s are shown in figure 8.

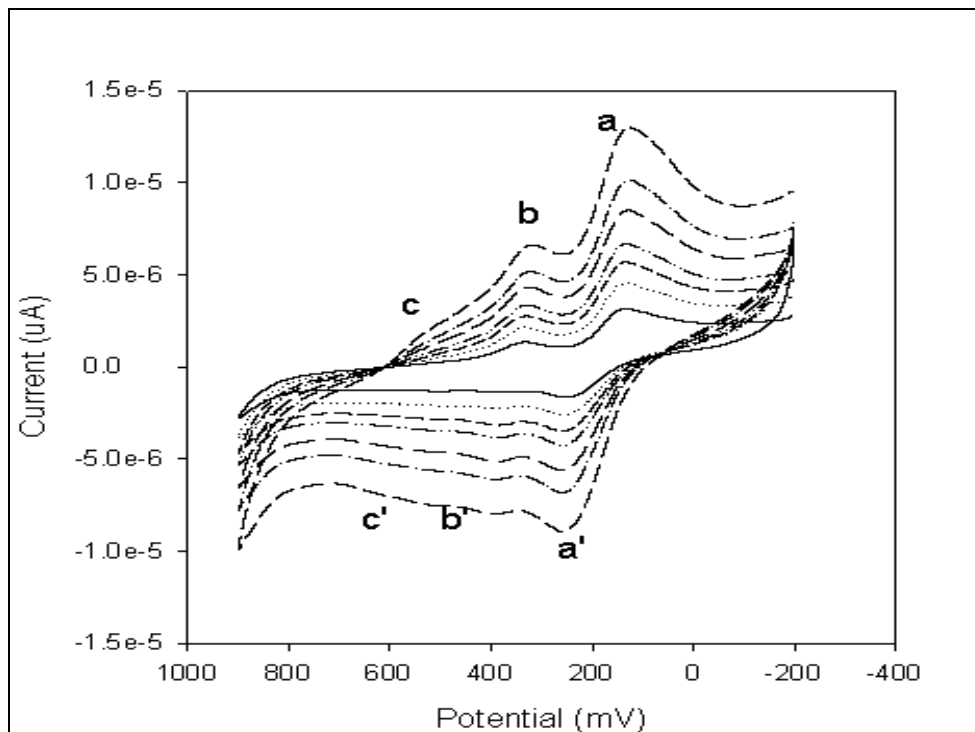


**Figure 8.** Multi-scan cyclic voltammograms (CV) of Pt/PANI-ASA in 1 M HCl at 25°C

Analysis of the voltammograms shows that the peak potentials and corresponding currents vary as the scan rates value varies. This indicates that the polymer nanotubes or fibres are electroactive and the electron transfer processes are coupled to a diffusion process namely, charge transportation along the polymeric nanostructures. Analysis of the cyclic voltammograms established 3 anodic and 3 cathodic peaks.

The redox peaks in the figure have been assigned using Pekmez formalism. The first oxidation peak represents polyleucoemeraldine radical cation (peak a') which is oxidized at more positive potentials to the half oxidized polymeraldine state (peak b') and then to the pernigraniline radical cation (peak c'). On the reversing potential, the pernigraniline (peak c) is first reduced to the polymeraldine radical cation (peak b) and finally to the fully reduced polyleucoemeraldine (peak a) [9, 27, 28].

Multi-scan rate voltammograms of PANI/PSA paste on Pt electrode in 1 M HCl with scan rates of 10, 20, 30, 40 and 50 mV/s are shown in figure 9.

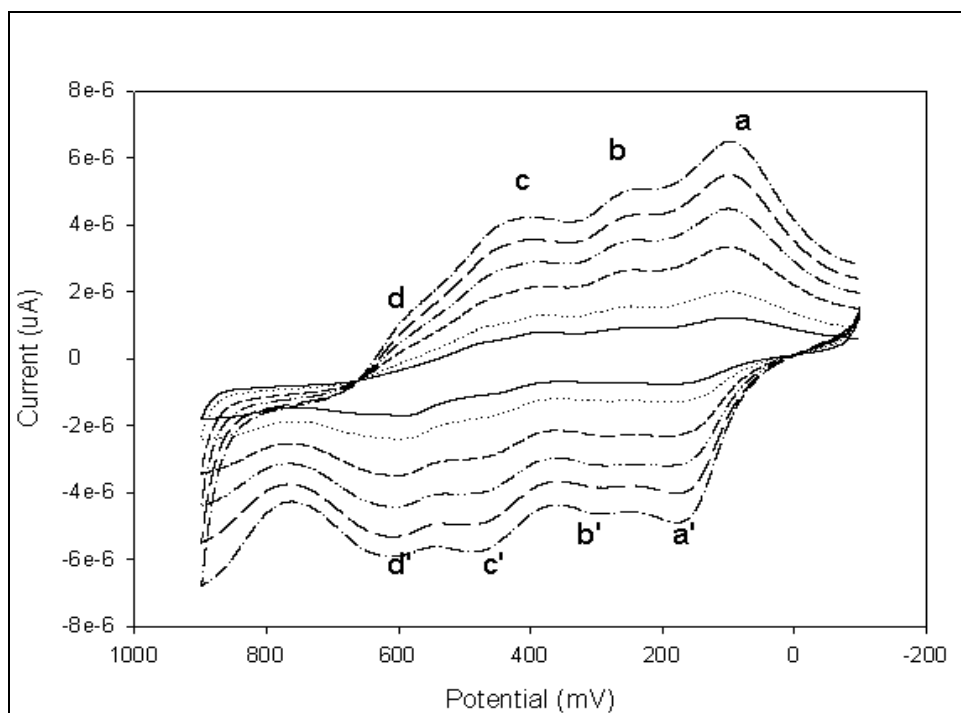


**Figure 9.** Multi-scan cyclic voltammograms (CV) of Pt/PANI-PSA in 1 M HCl at 25 °C

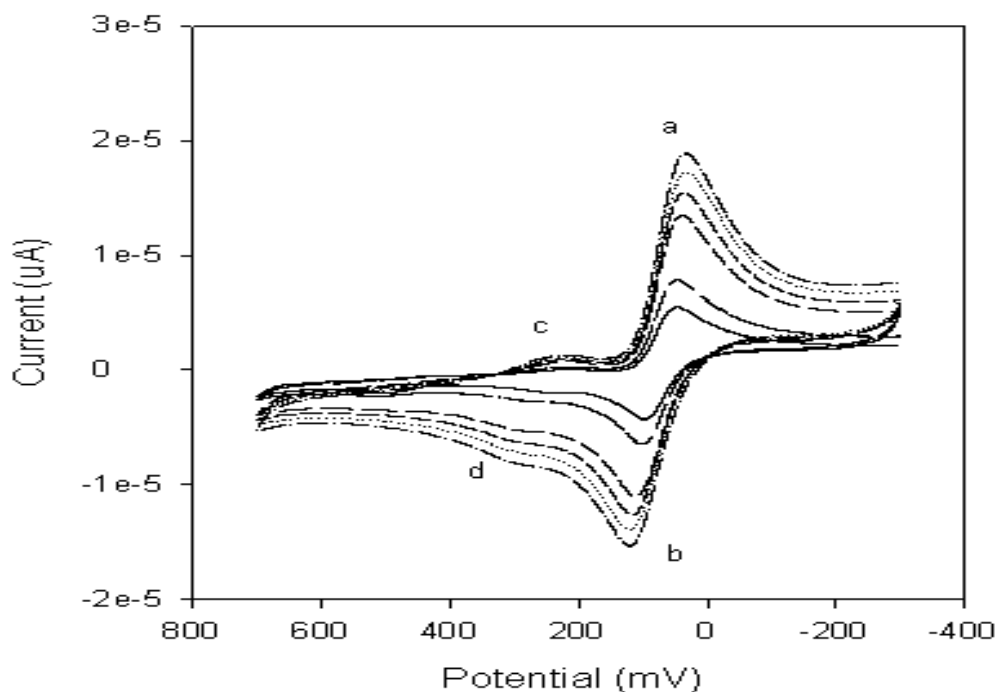


**Figure 10.** Multi-scan cyclic voltammograms (CV) of Pt/POMA-ASA in 1 M HCl at 25 °C

The peak potentials and corresponding currents also varies as the scan rates value varies. This proves that the PANI-PSA nanomaterials are electroactive and that charge transport along the polymer chain was taking place [27]. There are 4 anodic and 4 cathodic peaks in the voltammograms which

represents the same redox peaks as in PANI/ASA voltammograms with the inclusion of peaks d and d' that is generally attributed to the redox reaction of *p*-benzoquinone [28].

Figure 10 illustrates the multi-scan cyclic voltammograms obtained for POMA-ASA paste on a Pt electrode HCl (1 M) at different scan rates. It can be seen that there are 2 anodic and 2 cathodic peaks in the voltammograms. The shift of peak potentials and corresponding currents with scan rates indicated that the polymer nanomicelles are conducting and that hopping of electrons was taking place along the polymer structures. The first oxidation peak (peak b) at +101.7 mV is the emeraldine, which is further oxidized at higher potential to polyemeraldine radical cation at +274.8 mV (peak d). The cathodic peak scan is first reduced to the partly reduced leucoemeraldine radical cation at +216.1 mV (peak c), and then to the fully reduced leucoemeraldine (peak a) at +46.0 mV [29].

The multi-scan rate voltammograms of POMA-PSA paste on Pt electrode in HCl (1M) solution with scan rates 5, 10, 15, 30, 40 and 50 mV/s are shown in figure 11.

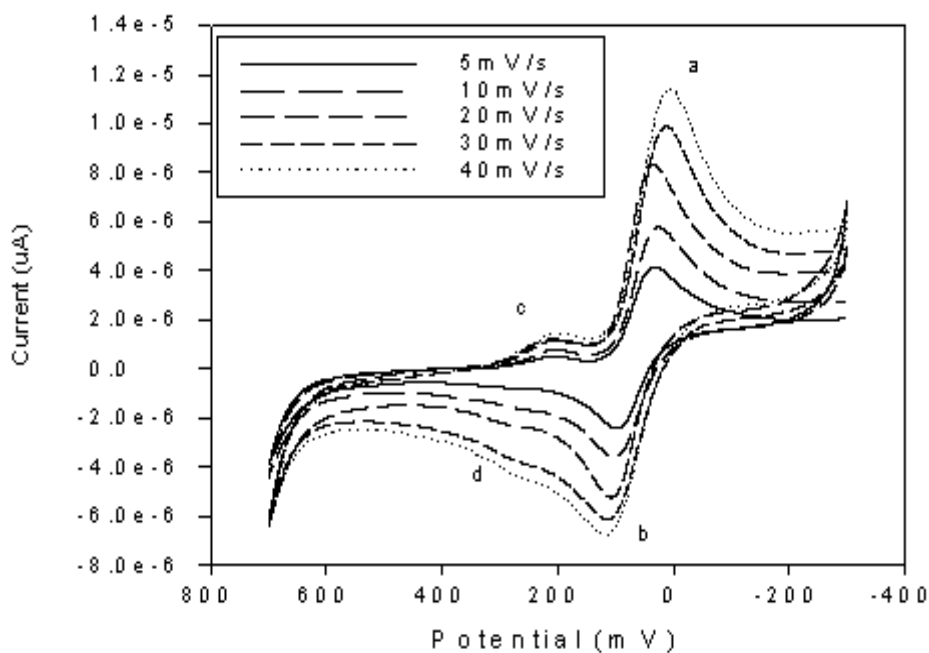


**Figure 11.** Multi-scan cyclic voltammograms (CV) of Pt/POMA-PSA in 1 M HCl at 25 °C

The peak potentials and corresponding currents are also seen to vary as the scan rates value varies. This indicated that the polymer nanomaterial structures are conducting and that diffusion of electrons was taking place along the polymer chain. The first oxidation peak at +113.4 mV is the emeraldine, which is further oxidized at higher potential to polyemeraldine radical cation at +268.9 mV. On the cathodic peak scan, polyemeraldine cation radical at +192.7 mV is reduced to the fully reduced leucoemeraldine at +10.8 mV [30].

Multi-scan rate voltammograms of PDMA-ASA on Pt electrode in HCl (1 M) with scan rates of 10, 20, 30, 40 and 50 mV/s are shown in figure 12.

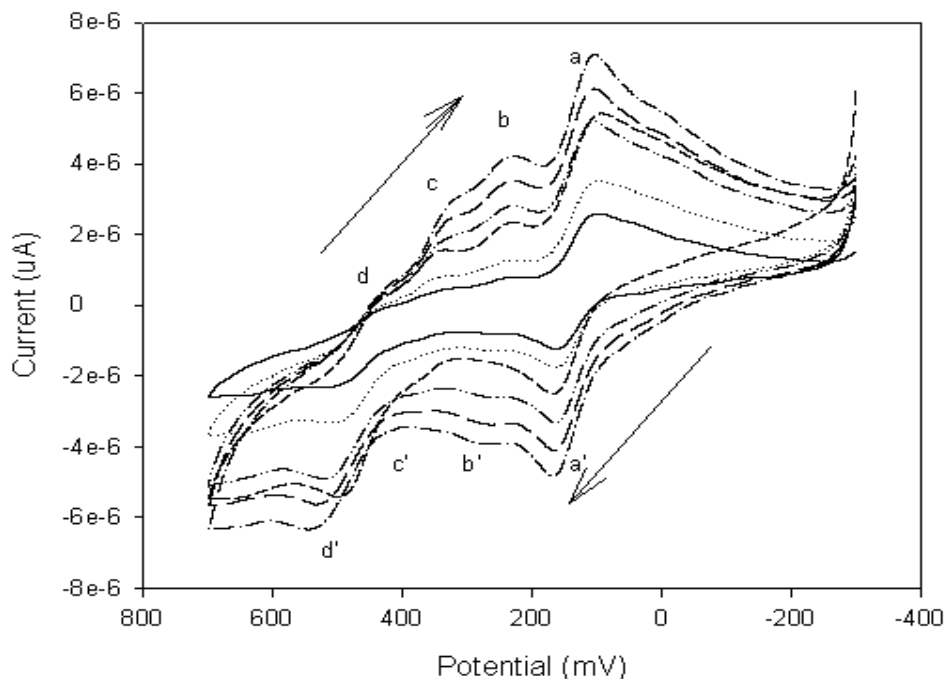


**Figure 12.** Multi-scan cyclic voltammograms (CV) of Pt/PDMA-ASA in 1 M HCl at 25 °C

The peak potentials and corresponding currents vary as the scan rates value varies. This confirmed that the polymeric nanowires are electroactive and that charge transport along the polymer chain was taking place [27]. It can be seen that there are 4 anodic and 4 cathodic peaks in the voltammograms. The first oxidation peak (peak a') at +163.3mV is due to the polyemeraldine state, which is further oxidized at higher potential to polyemeraldine radical cation at +268.9 mV (peak b□), which oxidized further to pernigraniline (peak c□) at +374.4 mV. For the cathodic scan, pernigraniline cation radical at +336.4mV (peak c) is first reduced to the partly reduced leucoemeraldine radical cation at +239.6mV (peak b), and then to the fully reduced leucoemeraldine (peak a) at +101.7mV. The redox couple d/d□ at approximately +500 mV is generally attributed to the redox reaction of *p*-benzoquinone [28]. The potentials of peaks b and a (reduced forms of the polymers) do not change as the scan rate was increased. This means that a surface bound species (stationary paste) was being used as a working electrode. No charge transfer accompanied the reduction process, only absorption. Peak a□, to a small extent, and peaks b□, c, c□ and d□ show increase in peak potential with scan rate. This shows charge transportation along the polymer chain and confirms that the polymer is conducting in its oxidised state [29-30].

Figure 13 illustrates multi-scan voltammograms of PDMA-PSA paste in HCl (1 M) with a Pt electrode with scan rates 5, 10, 15, 30, 40 and 50mV/s. Analysis of the voltammograms shows that the peak potentials and corresponding currents vary as the scan rate value vary. This indicates that the polymer nanowires are electroactive and the electron transfer processes are coupled to a diffusion process namely, charge transportation along the polymeric nanowires. Analysis of the cyclic voltammograms established 2 anodic and 3 cathodic peaks. The first oxidation peak at +224.1 mV is the emeraldine (peak a□), which is further oxidized at higher potential +477.0 mV (peak c□). On the

cathodic peak scan, pernigraniline cation radical at +354.0 mV (peak c) is reduced to the fully reduced leucoemeraldine at +119.3 mV (peak a) [13, 27, 28].

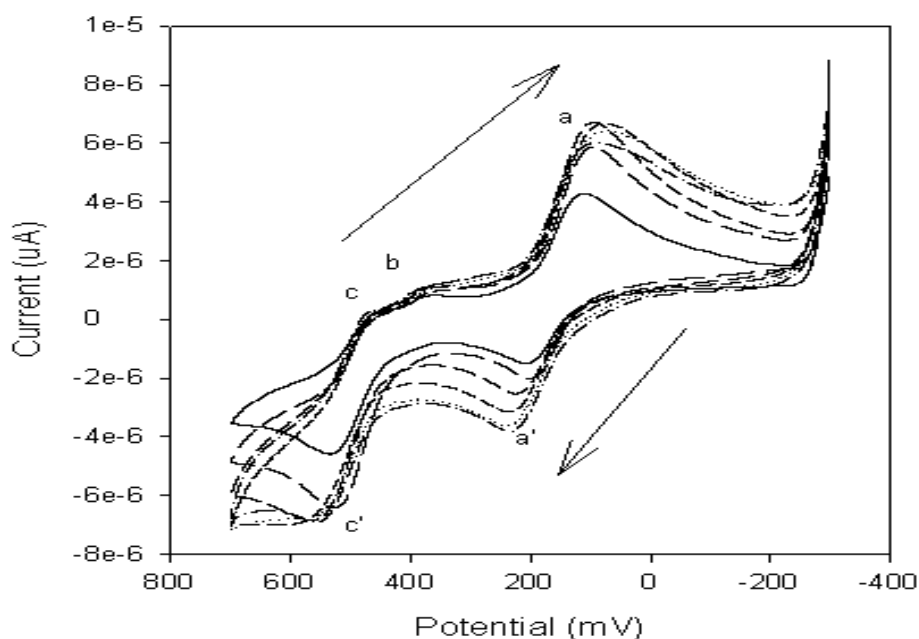


**Figure 13.** Multi-scan cyclic voltammograms (CV) of Pt/PDMA-PSA in 1 M HCl at 25 °C

### 3.2.2 Kinetic studies of the different polymers on Pt electrode in 1M HCl

The number of electrons transferred ( $n$ ) was estimated from the CV and was calculated for each of the polymers, using the formula

$$|E_p - E_{p1/2}| = 2.20 RT/nF = 56.5/n$$

and was found to be a one electron systems for all the polymers (Table 1).

The linear dependence of peak current on the scan rate for the various polymers, showed that we have a thin film of conducting electroactive nanotubes or nanomicelles immobilised on the electrode, which undergo rapid electron transfer reactions. This is typical of a Nernstian reversible reaction of a surface confine species. The surface concentration ( $\Gamma^* = \text{mol cm}^{-2}$ ) of the absorbed electroactive species could therefore be estimated from a plot of  $I_p$  versus  $v$  in accordance with the Brown Anson model [16]. The surface concentrations were seen to decrease in PANI > POMA > PDMA (table 1), which was due to the substituted methoxy groups in POMA and PDMA. On the other hand, the surface concentrations of polymers doped with PSA were higher than those doped with ASA, which was a result of the bulky angular PSA group compared with the bulky linear ASA group [31-33].

The Randel-Sevčik equation of analysis of voltammetric data was used to determine the rate of charge transport coefficient ( $D_e$ ) along the different polymer chains. The Randel-Sevčik behaviour of

the cyclic voltammetric peak currents has been used to evaluate  $D_e$  from the slope of the straight line obtained from the  $I_p$  versus  $v^{1/2}$  [31-33]. There is a direct correlation between the bulkiness of the polymer substituents, the efficiency of the electron-hopping and the rate of electron diffusion along the polymer chain. The diffusion coefficient was seen to decrease in PANI > POMA > PDMA (table 1) which was caused by the substituted methoxy groups that increases the inter-chain distance between the polymer units and thus impede electron-hopping across the units and was in accordance with [9] and [20].

The diffusion coefficient of polymers doped with ASA was faster than those doped with PSA. This was due to the steric hindrance emanating from the bend bulky PSA that increased the inter-chain separation and decreased frequency electron-hopping, compared to straight bulky ASA. These findings were further confirmed by calculation of the standard rate constant ( $k^0$ ), which was better along PANI > POMA > PDMA (table 1) [31-33].

The standard heterogeneous rate constant was higher for PDMA/ASA compared to the other polymers as seen in table 1. Mathebe et al. and Iwuoha et al. reported similar values for  $\Gamma^*$ ,  $D_e$  and  $k^0$  for electroactive polymers of PANI and PANI/PVS in 1M HCl, respectively [9, 27].

**Table 1.** Kinetic parameters for the conducting nanostructured polymers

Conducting nano-structured Polymer	Surface conc. $\Gamma^*$ (mol/cm <sup>2</sup> )	Diffusion coeff. ( $D_e$ ) cm <sup>2</sup> /s	Standard rate constant ( $k^0$ ) cm/s
PANI-ASA	$8.093 \times 10^{-3}$	$3.48 \times 10^{-6}$	$1.2 \times 10^{-3}$
PANI-PSA	$4.29 \times 10^{-3}$	$7.0983 \times 10^{-7}$	$6.042 \times 10^{-4}$
POMA-ASA	$4.629 \times 10^{-2}$	$1.0994 \times 10^{-8}$	$2.9255 \times 10^{-5}$
POMA-PSA	$9.679 \times 10^{-2}$	$5.4114 \times 10^{-9}$	$8.8875 \times 10^{-7}$
PDMA-ASA	$1.231 \times 10^{-2}$	$2.429 \times 10^{-7}$	$1.557 \times 10^{-4}$
PDMA-PSA	$2.960 \times 10^{-2}$	$2.008 \times 10^{-9}$	$5.593 \times 10^{-5}$

#### 4. CONCLUSIONS

It can be concluded that nanostructured conducting polyaniline (PANI), poly(*ortho*-methoxyaniline) (POMA) and poly(2,5 dimethoxyaniline) (PDMA) doped with anthracene sulfonic acid (ASA) and phenanthrene sulfonic acid (PSA) can be synthesised chemically. All polymers studied exhibited quinoid and benzoid bands typically of polyaniline FTIR-spectra which confirmed the polymers were formed. The presence of the sulfonate functionality suggested that the ASA and PSA groups were incorporated into the polymer backbones. Furthermore, UV-vis bands and shifts also showed that ASA and PSA were incorporated into the polymer backbones. SEM micrographs showed different nano-structured morphologies for the polymers, which include nano-tubes/fibres (PANI-ASA and PANI-PSA), nano-micelles or nano-sheets (POMA-ASA and POMA-PSA) and nano-wires (PDMA-ASA and PDMA-PSA).

Cyclic voltammetric characterisation of the polymer pastes showed distinctive redox peaks, which prove that the polymer films on the Pt electrode were electroactive and conductive and exhibit reversible electrochemistry. Thus, applying appropriate potential, the conductive nanostructured polymers can be stabilised at required oxidation states. These results support the view that conducting nanostructured polymers could prove promising for developing novel electro-catalysts for use in sensor devices.

#### ACKNOWLEDGEMENTS

This work was financially supported by the National Research Foundation (South Africa). The authors also would like to thank Dr. Miranda Wallace of the Microscopic Units at the University of Cape Town and Dr. Gerald Malgas of the University of the Western Cape.

#### References

1. H. Habermeier. *Mater. Science & Engin.* A199 (1995) 69.
2. L.A. Dobrzański, *J. of Mater. Proces. Technol.* 175 (2006) 133.
3. M. Manoharan. *Technol. in Soc.* 30 (2008) 401.
4. C. Johans, J. Clohessy, S. Fantini, K. Kontturi, V.J. Cunnane, *Electrochem. Commun.* 4 (2002) 227.
5. A.R. Hopkins, R.A Lipeles, W.H. Kao, *Thin Solid Films* (2004) 474.
6. Z. Zhang, M. Wan, *Synth. Met.* 128 (2002) 83.
7. Z. Zhang, M. Wan, *Synth. Met.* 132 (2003) 205.
8. M. Mazur, M. Tagowska, B. Palys, K. Jackowska, *Electrochem. Commun.* 5 (2003) 403.
9. E.I. Iwuoha, D.S. de Villaverde, N.P. Garcia, M.R. Smyth, J.M. Pingarron, *Biosens. and Bioelectr.* 12 (1997) 749.
10. H.J. Qiu, M.X. Wan, *Mater. Phys. Mech.* 4 (2001) 125.
11. M.G. Han, S.K. Cho, S.G. Oh, S. S. Im, *Synth. Met.* 126 (2002) 53.
12. Vogel AI, in *Vogel's Text Book of Practical Organic Chemistry*, 5<sup>th</sup> Ed, Wiley, New York, 1989
13. M. Wan, Z. Wei, Z. Zhang, L. Zhang, K. Huang and Y. Yang, *Synth. Met.*, 135-136 (2003) 175.
14. P. Sbaite, D. Huerta-Vilca, C. Barbero, M. C. Miras and A. J. Motheo, *European Polym. J.*, 40 (2004) 1445.
15. S. Patil, J. R. Mahajan, M. A. More and P. P Patil, *Mater. Science & Engin.*, B87 (2001) 134.
16. M. R. Fernandes, J. R. Garcia, M. S. Schultz and F. C. Nart, *Thin Solid Films* 474 (2005) 279
17. A. Malinauskas and R. Holze., *Synth. Met.*, 97 (1998) 31
18. Z. Zhang, Z. Wei, L. Zhang and M. Wan, *Acta Materiala*, 53 (2005) 1373
19. Y. Wei, W. W. Focke, G. E. Wnek and A. Ray, A.G MacDiarmid, *J. Phys. Chem.*, 93(1989) 495
20. M. Karakisia, M. Sakac, E. Erdem and U. Akbulut, *J. of Appl. Electrochem.*, 27 (1997) 309
21. L.Huang, T.Wen, A.Gopalan, *Synth. Met.* 130 (2002) 155.
22. L.Huang, T.Wen, A.Gopalan, *Mater. Chem. & Phys.* 77 (2002) 726.
23. J. Widera, B. Palys, J. Bucowska and K. Jackowski, *Synth. Met.*, 94 (1998) 265
24. F. Cataldo and P. Maltese, *European. Polym. J.*, 38 (2002) 1791
25. L. Zang and M. Wan, *Thin Solid Films* 24 (2005) 477
26. W.A.Gazotti, M. dePaoli, *Synth. Met.* 80 (1996) 263-269
27. N. G. R. Mathebe, A. Morrin and E. I. Iwuoha, *Talanta* 64 (2004) 115-12
28. A.J Bard and L.R Faulkner, *Electrochemical Methods: Fundamentals and Applications*, 2<sup>nd</sup> ed., Wiley, New York (2001)
29. J. C. Chiang, and A. G. MacDiarmid, *Synth. Met.*, 13 (1986) 193

30. A. G. MacDiarmid, J. C. Chiang, A. F. Richter and A. J. Epstein, *Synth. Met.*, 18 (1987) 285
31. P. Monk, *Fundamentals of Electro-Analytical Chemistry*, Chichester: John Wiley & Sons Ltd (2001)
32. P. Zanello, *Inorganic Electrochemistry. Theory, Practice and Application* Cambridge, UK: The Royal Society of Chemistry (2003)
33. T. J. Kemp, and Southampton Electrochemistry Group In., *Instrumental Methods in Electrochemistry*, Ellis Horwood Ltd: Chichester, (1990)

© 2012 by ESG ([www.electrochemsci.org](http://www.electrochemsci.org))